Modeling The Hyperloop With COMSOL Multiphysics®: On The Aerodynamics Design Of The EPFLoop Capsule

Nicolò Riva[1], Lorenzo Benedetti[2], Zsófia Sajó[3]

EPFL and EPFLoop, [1]*SCI IC BD - Applied Superconductivity STI*, [2]*GEL - GeoEnergy Laboratory ENAC*, [3]*M.Sc. Student in Materials science STI*

Abstract: The EPFLoop team from Ecole Polytechnique Fédérale de Lausanne has developed a capsule thanks to which it won the 3rd place in SpaceX's Hyperloop Pod Competition in 2018. COMSOL Multiphysics was used to analyze and study the aerodynamics of the pod.
The conditions at which the pod is designed require the consideration of compressible flow (meaning Mach Number $M_a > 0.3$). Consequently, simulations were performed using the High Mach Number Flow (HMNF) solver. Preliminary 2D analyses were carried out as a first attempt at shape optimization, using the LiveLink™ for MATLAB®, and a Genetic Algorithm developed by EPFLoop. Then, the 3D design was studied under turbulent stationary conditions.
This project requires the aeroshell to be both lightweight and withstand the design load conditions given by the deceleration (2.6g) and the pressure maps obtained by the CFD simulations. Therefore, a composite aeroshell was studied using a stack of shell finite element models to represent the various layers. A curvilinear coordinate interface was used to define the properties of the anisotropic material on a complex geometry. During the iterations on the design, critical spots were identified. Hence, the aeroshell has been reinforced locally with ribs and unidirectional layers. The result is a light and strong aeroshell of about 8 kg, manufactured by the LPAC laboratory at EPFL.

Keywords: Hyperloop, SpaceX, EPFL, EPFLoop, Composites, Carbon Fiber, CFD, competition

1. Introduction

The concept of Hyperloop Alpha concept has been proposed in an open source paper published by Elon Musk and SpaceX [1], as a passenger or goods high-speed rail system. The Hyperloop can satisfy a growing need of transportation on short-middle travel. For instance, on the Bern-Zürich (123 km) route the traveling time can be reduced to 9 minutes. The Hyperloop Pod Competition, created by SpaceX in 2015, aims to encourage innovation and to improve the development of a working prototype. This work describes how the EPFLoop team used COMSOL Multyphysics to analyze and study the design of the aerodynamic systems of their prototype, which allowed to win the third place in the SpaceX Hyperloop competition 2018.

The optimization of the aeroshell's shape in order to guarantee the highest possible acceleration has been done using a CFD stationary analysis. The aeroshell should be both lightweight and withstand the maximum acceleration and deceleration during the run. Therefore, a composite aeroshell was chosen and was studied using a structural stationary analysis.

2. Governing equation and design approach

a. CFD analysis: compressible flow regime in stationary solution

Despite the extremely low pressure in the Hyperloop tube (861 Pa) and, hence, the low density of air, aerodynamic forces should be considered, since the EPFLoop pod will be targeting a maximum speed of 134 m/s. The EPFLoop team proceeded with iterative steps, changing the aeroshell shape and evaluating the associated improvements with the CFD modules. First, the approximated Reynolds range for the prototype is computed. The characteristic length is assumed to be represented by the length of the Pod whereas the density and the viscosity are respectively 0.0103 kg/m^3 and $1.846 \cdot 10^{-5}$ Pa·s. The Reynolds number reads:

$$R_e = \frac{\rho V L}{\mu} = 262540 \qquad (1)$$

Hence, turbulent effects cannot be neglected and the turbulence model choice in the CFD software are of great importance. In these conditions, the speed of the sound is $S = 343$ m/s. The Mach number is:

$$M_a = \frac{v}{S} = 0.38 \qquad (2)$$

Being that $M_a > 0.3$, compressibility effects start to be not negligible. The expected drag is computed assuming high Reynolds number (R_e>1000) as:

$$F_D = \frac{1}{2} C_D A v^2 \qquad (3)$$

where C_D is the drag coefficient, A the cross section of the Pod, and v the velocity of the pod. The time dependent Navier-Stokes equations for compressible flow are solved to obtain the steady state solution. In particular, the High Mach Number Flow module is used, both for 2D and 3D. The FEM solver employs a

non-conservative form of the governing equations as described below [2]:

$$\frac{\partial \rho}{\partial t} + \rho \cdot \boldsymbol{\nabla} \cdot (\mathbf{u}) + (\mathbf{u} \cdot \boldsymbol{\nabla})\rho = 0 \quad (4)$$

$$\rho\left(\frac{\partial \mathbf{u}}{\partial t} + (\mathbf{u} \cdot \boldsymbol{\nabla})\mathbf{u}\right) = \boldsymbol{\nabla} \cdot \left[-p \cdot \boldsymbol{I} + \mu \cdot \left((\boldsymbol{\nabla}\mathbf{u}) + (\boldsymbol{\nabla}\mathbf{u})^T - \frac{2}{3} \cdot \boldsymbol{\nabla} \cdot \mathbf{u} \cdot I\right)\right] \quad (5)$$

$$\rho \cdot C_p\left(\frac{\partial \mathrm{T}}{\partial t} + (\mathbf{u} \cdot \boldsymbol{\nabla})\mathrm{T}\right) = \boldsymbol{\nabla} \cdot (\mathrm{k} \cdot \boldsymbol{\nabla}\mathrm{T}) + \frac{T}{\rho} \cdot \left(\frac{\partial \rho}{\partial T}\right)_p \left(\frac{\partial p}{\partial T} + (\mathbf{u} \cdot \boldsymbol{\nabla})p\right) + \boldsymbol{\nabla}\boldsymbol{u} : \left[\mu \cdot \left((\boldsymbol{\nabla}\mathbf{u}) + (\boldsymbol{\nabla}\mathbf{u})^T - \frac{2}{3} \cdot \boldsymbol{\nabla} \cdot \mathbf{u} \cdot I\right)\right] \quad (6)$$

Ideal gas conditions are considered meanwhile the viscosity-temperature coupling is taken into account by Sutherland's law [2]:

$$\mu = \mu_{ref}\left(\frac{T}{T_{ref}}\right)^{\frac{3}{2}}\left(\frac{T_{ref}+S}{T+S}\right) \quad (7)$$

The thermal conductivity k is directly obtained from the material library in COMSOL.

b. Structural analysis: failure prediction of the carbon fiber aeroshell

The structural behavior of the composite carbon fiber aeroshell is described using shell finite elements, representing the various plies of material. The analysis is carried out under plane stress assumptions and stationary conditions.
If the stress in the shell is represented by the tensor σ, then the equilibrium equation is described by:

$$\nabla \cdot \sigma + F_v + 6(M_v \times n)\frac{z}{d} = 0 \quad (8)$$

where z is the local coordinate through the thickness of the shell, d is the thickness, n is the normal to the shell and F_v and M_v are respectively the applied force and moment to the shell. In turn, the stresses are defined from the Green-Lagrange strains as function of the degrees of freedom displacement u and rotation a [3]. In order to take into account the contribution of various plies, u and a are shared between all the plies. Moreover, the orientation of the fibers is defined by the local axis reference, which allows to define precisely the distribution and characteristics of the layers.

The carbon fiber-epoxy plies were modelled assuming an orthotropic material. For this type of material, a quadratic failure criterion may be introduced [4] and, in its general form reads:

$$f(\Sigma) = a_{ij}\sigma_{ij} + b_{ijkl}\sigma_{ij}\sigma_{kl} \leq 1 \quad (9)$$

where $f(\Sigma)$ is the expression built on the stress tensor Σ, a and b are experimentally determined material strength parameters.
The Tsai-Wu criterion is part of this category. It is used in the case of plane stress: the stress is located in the plane identified by the axes of orthotropy l and t, parallel to the ply. This assumption is valid for thin shells, i.e. its thickness is significantly smaller that its length and width. The Tsai-Wu failure criterion expression reads:

$$a_{ll}\sigma_l + a_{tt}\sigma_t + B_l\sigma_l^2 + B_t\sigma_t^2 + B_o\sigma_l\sigma_t + B_{lt}\tau_{lt}^2 \leq 1 \quad (10)$$

where σ_l and σ_t are failure strength values, and B_o is a coupling term used to optimize the orientation of the ellipsoid constituting the failure envelope in axes (σ_l , σ_t , τ_{lt}). The default value of B_o is -1 [4].
Similarly, each principal stress in the fiber was considered and compared to their respective strength. Hence, the failure criterion reads:

$$f(\Sigma) = \frac{\hat{\sigma}_i}{\hat{a}_i} \leq 1 \quad (11)$$

where $\hat{\sigma}_i$ is the principal stress and $\hat{a}_i$ is the strength in the i-th direction. The Tsai-Wu safety factor and principal stresses failure criterion was useful to determine the structural strength for the given configuration of plies. In addition, in order to avoid any interference between the deformation of the aeroshell and the other components of the pod, the total displacements are computed and compared to the maximum clearance available.

3. 2D iterative design based on genetic algorithms and 3D design

The optimization phase is one of the most important during the design of a performant device. Due to the timeline, the EPFLoop team could not define the entire design based on an optimized solution, but instead used optimization as an improvement of the initial design. These techniques can be applied to a wider set of problems, e.g. chassis design, power distribution. The idea is to use an iterative evolutionary algorithm, generating a succession of converged solutions $\{s_k\}$, which must satisfy given requirements. In a design optimization problem, the biggest issue is to link the objective function to a geometrical parameter and proper constraints.

In 2D, the total aerodynamic force is computed as a line integral along the longitudinal cross section of the aeroshell on the central plane of symmetry (Fig. 3.1). Note that on the symmetry plane, where the flow is initially simulated, some physics, which is typical of 3D simulations, is missing. The functions

to minimize are identified as the ones of drag and lift coefficients, that are:

$$C_D A = 2F_D A v^2 \quad (12)$$

$$C_L A = 2F_L A v^2 \quad (13)$$

No single solution exists that simultaneously optimizes each objective function. Therefore, one should first approximate or compute all or a representative set of Pareto optimal solutions for that problem [5]. For this work, a GA previously used for the design of a superconducting devices has been employed [6]. The initial solution is the longitudinal cross section on the symmetry plane of the 2D simulation. The bottom part of the aeroshell is fixed, meanwhile the upper part is composed by 3 Bezier curves of 3rd order. The points of such curves are the values to be optimized.

a. 2D design in subsonic compressible flow with optimization based on GA

Geometry of the aeroshell

The preliminary design of the profile of the shell has been done to ensure a complete enclosure of the subcomponents of the Pod (Fig. 3.1).

Boundary condition and solver

The settings chosen for the numerical flow simulation study in COMSOL are summarized in Table 3.1. The module used is the HMNF (High Mach Number Flow), coded for situations where $M_a > 0.3$.
The set criteria convergence of 10^{-4}, for the non linear solver has been reached after ~200 iterations. A larger distance from the domain boundaries was considered behind the Pod ($\sim 3 \cdot L_{POD}$) than in front of it ($\sim 1 \cdot L_{POD}$) in order to have enough space to study the wake region. An overview of the computational domain and of boundary conditions can be found in the Fig. 3.2 below. The boundary conditions are a speed inlet, pressure outlet, the symmetry plane, a no slip condition on the Pod, and slip conditions on the tube.

Table 3.1 - CFD settings in COMSOL.

Parameter	Setting
Solver	Density based, Segregated Steps
Turbulence model	k-ϵ with standard wall function
Fluid	Air with density based on ideal gas law
Initialization	Standard, from inlet
Solution methods	Algebraic Multigrid
Solution controls	Speed and Turbulence

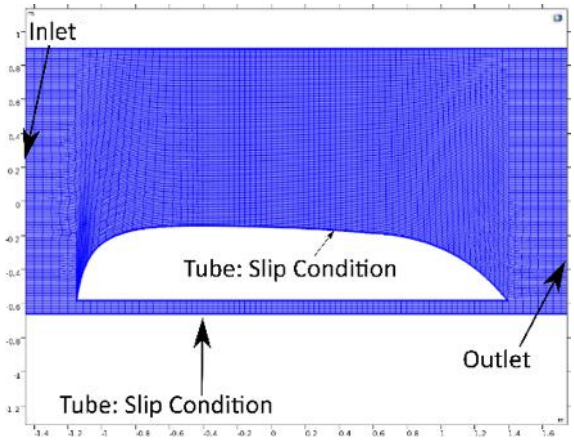

Figure 3.2 - Computational domain.

Mesh

As the flow is characterized by an incident shock wave, structured quad mesh is implemented as mesh to capture this effect. The physics of the model allows also to evaluate the boundary layers effects.

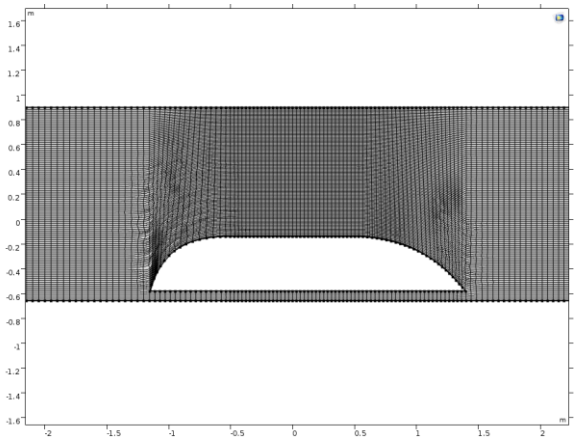
Figure 3.2 - Non optimized mesh.

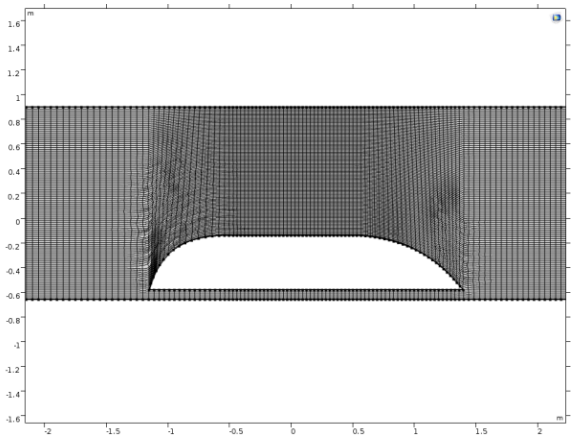
Figure 3.3 - Optimized mesh.

Results

In Fig. 3.4 and Fig. 3.5, the computed pressure contour maps and the optimized drag coefficient of the non-optimized and optimized solution. The difference lays on a better recirculation of the air on the back and, consequently, a lower C_D, which values are in the captions of Figures. 3.4 and 3.5.

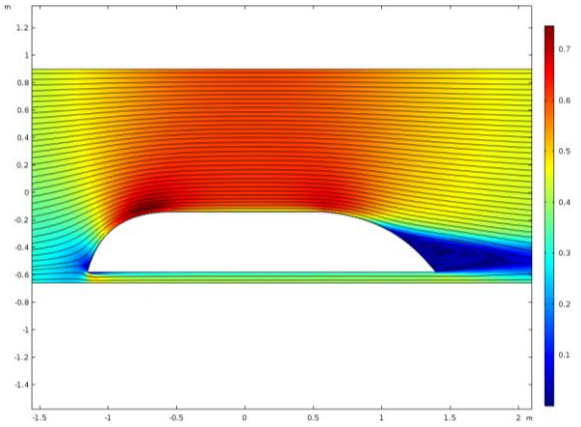

Figure 3.4 - Non optimized solution. Surface: Mach number, streamline: velocity field. $C_D A = 0.1657$

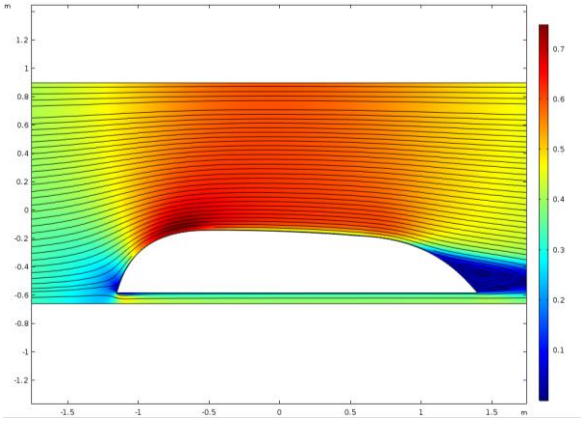

Figure 3.5 - Optimized solution. Surface: Mach number, streamline: velocity field. $C_D A = 0.147$

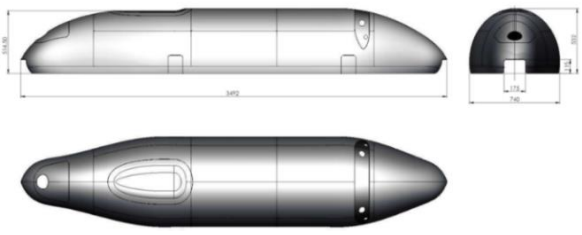

Figure 3.6 - Final aeroshell design.

b. 3D design validation in subsonic compressible flow

Geometry of the aeroshell

The final design of the aeroshell is presented in Figure 3.6.

Boundary condition and solver

The settings chosen for the numerical flow simulation study on COMSOL are the same of the case in 2D.

The continuity residuals and the scaled species residuals were of the order of 10^{-4} after ~200 iterations.

An overview of the computational domain and boundary conditions can be found in the Fig. 3.7 below. The boundary conditions are a speed inlet, pressure outlet, the symmetry plane, a no slip condition on the Pod, and slip conditions on the tube.

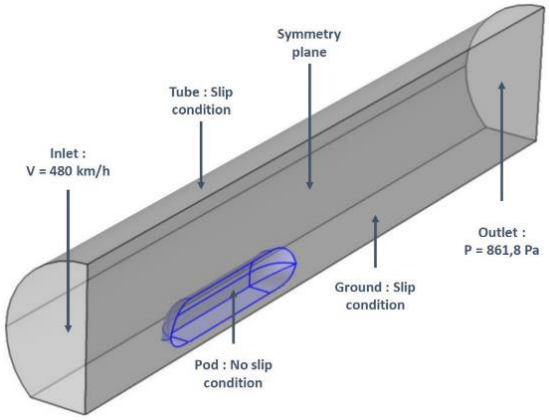

Figure 3.7 - Representation of the computational domains and condition.

Mesh

As the flow is characterized by high Mach number, to capture the shock waves and the boundary layers effects, a quadratic mesh is implemented. The boundary layer thickness and growth rate are applied on both slip and no-slip walls. Based on an invariance study (see Table 3.5), the produced mesh is depicted in Fig. 3.8. The surfaces where capturing the correct fluid flow is more crucial are characterized by a very fine Hexahedral mesh.

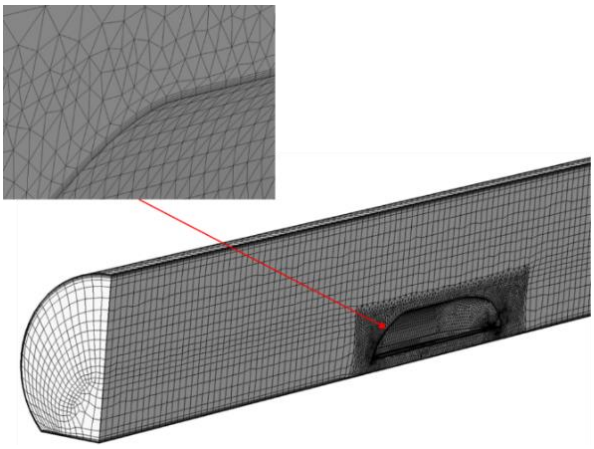

Figure 3.8 - COMSOL volume mesh for $0.5 \cdot 10^6$ elements.

Figure of merit

The lift and drag coefficients for the Pod were estimated from the numerical simulations. Two scenarios were considered: one is under normal operating conditions (861 Pa) and another in case of rapid pressurization of the Hyperloop tube (101325 Pa). The reference values used for calculating the aerodynamic coefficients are given in Table 3.3.

Table 3.3 – Simulation parameters.

$A[m^2]$	$v[m^2]$	$\rho_{nom}[kg/m^3]$	$\rho_{ATM}[kg/m^3]$
0.17854	134	0.0103	1.12123

where v is the speed, A the cross section and ρ the density at a given pressure. The forces F_L and F_D are the respectively the total viscous and pressure forces. The forces are obtained by calculating the surface integral of the viscous and pressure stress T_z and T_x (equations 12 and 13). The results are given in Table 3.5.

Table 3.4 - Force values at design and atmospheric pressure. Second iteration design.

	Lift [N]	Drag [N]	C_L	C_D
Design Condit. (861Pa)	0.362	4.380	0.040	0.270
Tube Breach (101325 Pa)	48.386	352.290	0.027	0.199

Results

To determine the aerodynamics coefficients on the Pod, a grid invariance study has been performed. Table 3.5 reports the results:

Table 3.5 – Results of the grid invariance study.

Number of elements	$0.5 \cdot 10^6$	10^6	$2.3 \cdot 10^6$
Lift (N)	0.356	0.362	0.335
Drag (N)	4.335	4.3803	4.2546

The residual values for the simulations in COMSOL are below $1 \cdot 10^{-3}$ for $0.5 \cdot 10^6$ and $1 \cdot 10^6$ elements and below $1 \cdot 10^{-4}$ for $2.3 \cdot 10^6$ elements (Table 3.5). On an Intel Xeon CPU E5430@2.66 GHz, with 32GB or RAM, the computation time took about 12 h for the $0.5 \cdot 10^6$ elements simulation, about 23h for the $1 \cdot 10^6$ elements simulation and about 60h for $2.3 \cdot 10^6$ elements.

In the results, a stagnation zone is visible at the front of the Pod (Fig. 3.9). A vortical flow is observed at the separation zone. At the rear of the pod a significant change in pressure is present as the separation region affects the sides of the pod, far from the plane of symmetry (Fig. 3.9). The local Mach number does not exceed 0.5 in the domain (Fig. 3.10).

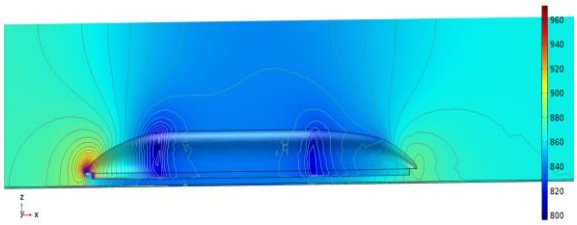

Figure 3.9 - Absolute pressure on the pod.

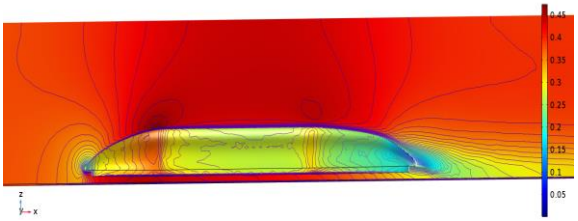

Figure 3.10 - Contour plot of Mach number.

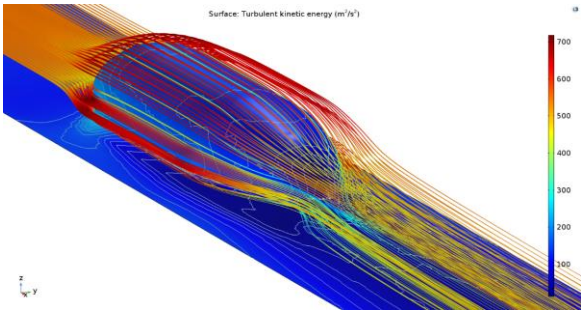

Figure 3.11 - Streamline representing the speed components, their radius is proportional to TKE. On the floor and pod surface, TKE is plotted.

4. 3D structural analysis of the aeroshell

The composite aeroshell is required to withstand the acceleration, deceleration and aerodynamic pressure loads during the run in vacuum. As requested by SpaceX, the aeroshell structure should provide a safety factor of 2 under load and at all points.

Carbon fiber and epoxy composites are strong, yet lightweight, which make them ideal for applications

in high-acceleration uses, such as the Hyperloop. A sandwich structure adds rigidity to the structure. However, to optimize the weight, a local sandwich structure using foam ribs was preferred to a reinforcement of the whole structure with a foam layer. Flax fibers were added to the inside of the aeroshell to enhance rigidity on the whole surface.

a. Geometry, mesh, solver and settings

The geometry of the aeroshell has been extracted from the optimization procedure previously described. In order to take into account the carbon fiber epoxy composite's anisotropy, combined with the complex geometry of the aeroshell, a curvilinear coordinate has been used to define the orientation of load and the mechanical properties. The curvilinear coordinate interface was created in COMSOL using rotated coordinate systems for each carbon fiber ply. Additional plies for reinforcement were added by subdividing the geometry of the 2D surface in multiple domains. In particular, it is possible to observe the front and back sandwich ribs and the central X-shaped reinforcement.

A stationary simulation was used in this analysis: the situation of interest takes place at the moment of the highest deceleration (2.6 g). The load is represented by the pressure map obtained from the CFD simulations and during the inertia of the mass of the aeroshell (Fig 3.9).

The quality of the mesh, a combination of free triangular and mapped triangular elements, was measured using skewness, which was close to 1 on most of the computational domain (Fig. 4.1).

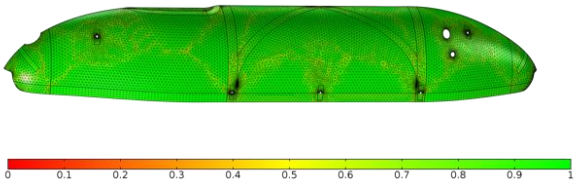

Figure 4. 1 - Free triangular and mapped mesh : quality measured using skewness.

b. Structural analysis of a stack of carbon fiber layers

As a starting point, a stack of various plies in the shape of the aeroshell was modelled using shell finite elements. The weakest points were then reinforced with more plies and foam ribs, aiming at reducing the final weight of the structure.

In COMSOL, prescribed displacements were applied to the boundaries where attachments are glued on the real pod, to ensure the link between the aeroshell and the chassis.

c. Results

The behavior of the aeroshell was validated through the study of principal stresses, the Tsai-Wu failure criterion and the total displacement. The principal stresses (Fig. 4.2) were found to be concentrated at the attachments. In these areas, the high stress is due to the prescribed displacement and the applied load given by the deceleration. The stress distribution shows a global compressive state in the top layer, whereas an arch-like resisting structure is observed to develop along the center and the edges of the aeroshell. In addition, tensile efforts are limited, being their maximum an order less than the compression ones. The stress was also observed to be significant in the vicinity of the middle of the shell. Along these axes, unidirectional reinforcements were placed in order to reduce the stress in the shell. Foam was placed on the front and back of the aeroshell to increase rigidity, as the total displacement is the highest in these areas: up to $7.43 \cdot 10^{-4}$ m. (Fig. 4.3). The additional reinforcements have also the beneficial effect of reducing the load in the central part of the structure and, consequently, avoiding local buckling phenomena.

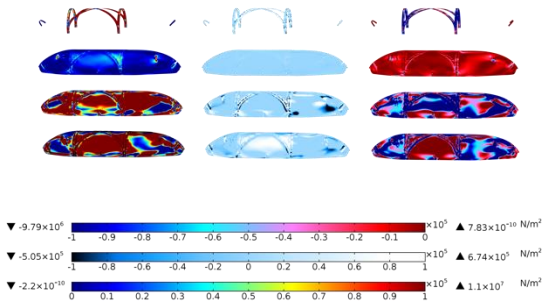

Figure 4.2 - First, second and third principal stresses (left to right) in the unidirectional carbon fiber and foam reinforcements, flax fiber net, inner and outer bidirectional carbon fiber shell (top to bottom).

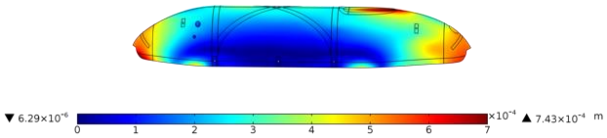

Figure 4.3 - Total displacement of the aeroshell.

In the resulting structure, the Tsai-Wu safety factor was at least of 2 at every point of the aeroshell (Fig. 4.4).

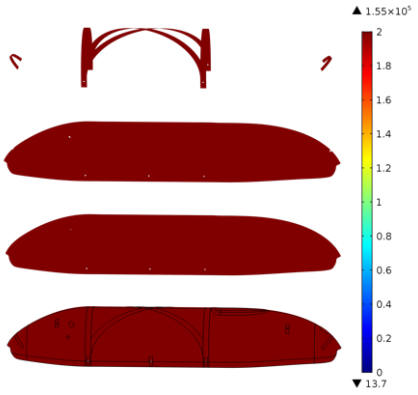

Figure 4.4 - Tsai-Wu safety factor (middle): unidirectional carbon fiber and foam reinforcements, flax fiber net, inner and outer bidirectional carbon fiber shell (top to bottom).

The weight of the aeroshell calculated based on the COMSOL simulation was approximately 8 kg. The aeroshell based on these computations was manufactured by the LPAC laboratory at EPFL.

5. Conclusion

The EPFLoop team succeeded in studying and developing the optimal shape and composite structure of the aeroshell using CFD and structural stationary analyses. This work pointed out how interdisciplinary and polyhedral skills can lead to new solutions in science and engineering. EPFLoop, thanks to COMSOL and other partners, will continue its work for the 2019 SpaceX Competition.

The authors would like to acknowledge the support of EPFL, FEE, COMSOL and the invaluable collaboration of LPAC – Laboratory for Processing of Advanced Composites (STI-EPFL) and Cyril Dénéréaz (LMM-STI-EPFL).

References

[1] SpaceX (2013). *Hyperloop Alpha*, SpaceX. (Online Article),http://www.spacex.com/sites/spacex/files/hyperloop_alpha.pdf,

[2] Amercan Institute of Aeronautics and astronautics (1998). *Guide for the Verification and Validation of CFD*

[3] Bathe K.J. (1996). *Finite element procedures*, Prentice-Hall, Englewood Cliffs, NJ

[4] Gay D. (2015). *Composite Materials Design and Applications*, Boca Raton, FL, CRC Press

[5] K. Miettinen. *Nonlinear Multiobjective Optimization*, Springer 1999

[6] N. Riva, R. Musenich et al. *Study of a Superconducting Magnetic Diverter for the ATHENA X-Ray Space Telescope*, IEEE Transactions on Applied Superconductivity (Volume: 28, Issue: 4, June 2018)